ADVANCED SENSOR RESEARCH Open Access
www.advsensorres.com

A Sensitive, Specific and Fast Electrochemical-based Nanobiosensor Diagnostic for *Xanthomonas albilineans*, the Cause of Sugarcane Leaf Scald Disease

Moutoshi Chakraborty, Shamsul Arafin Bhuiyan, Simon Strachan, Muhammad J.A. Shiddiky, Nam-Trung Nguyen, Narshone Soda, and Rebecca Ford*

Leaf scald (LS) caused by *Xanthomonas albilineans* (*Xalb*), is a major bacterial disease of sugarcane. The unreliable symptom expressions make traditional visual detection challenging. The molecular methods of detection require expensive equipment, labor-intensive, and time-consuming. This study proposes a novel electrochemical (EC)-approach, that is relatively easy to use and less expensive to detect *Xalb* DNA in LS-infected sugarcane leaves, meristematic tissue, and xylem sap samples. This method involves three key steps: i) DNA isolation from sugarcane samples via boiling lysis; ii) magnetic purification of target sequences from the lysate using magnetic bead-bound capture probes; and iii) EC detection of the target DNA. The method shows excellent detection sensitivity (10 cells μL^{-1}), reproducibility (Standard deviation, SD <5%, for $n = 3$), and a wide linear dynamic range (1 nM–1 fM or 10^6–10° copies μL^{-1}, $r = 0.99$). The EC assay has a strong negative correlation with quantitative polymerase chain reaction (qPCR) results ($r = -0.95$–0.97, $n = 24$, $p < 0.001$), and weak or no correlation with the varietal resistance ratings. This EC-based assay can be a commercially viable alternative, providing a DNA isolation/purification-free solution, and can potentially be adapted into a handheld device for on-farm detection and quantification of the LS-causing pathogen.

1. Introduction

Leaf scald (LS) is a major bacterial disease of sugarcane (*Saccharum* spp.), caused by the gram-negative, rod-shaped bacterium *Xanthomonas albilineans* (*Xalb*). This disease has been reported in over 66 sugarcane-producing countries, representing a significant global threat to sugar production.[1,2] In susceptible varieties, LS may result in considerable reductions in cane production and juice quality, leading to their removal from commercial production. LS may completely destroy whole sugarcane fields within a few months if susceptible cultivars are planted.[2]

Xalb multiplies in the xylem and spreads throughout the sugarcane plant, displaying distinctive symptoms like white, narrow, sharply defined leaf stripes that eventually lead to total leaf necrosis and wilting, and finally plant death.[3,4] The pathogen can remain undetected and latent in asymptomatic infected plants for several months, leading to sudden and severe epidemics. *Xalb* spreads primarily through contaminated harvesting equipment and infected cuttings from symptomless plants.[2] However, aerial transmission also occurs.[5,6] The most effective methods to manage leaf scald include pathogen diagnosis, hot water treatment, growing resistant cultivars, and the use of clean planting materials.[2]

Traditionally, detection of LS disease depends on observing phenotypic symptoms. However, the latent and variable expres-

M. Chakraborty, R. Ford
Centre for Planetary Health and Food Security (CPHFS)
Griffith University
Nathan Campus, QLD 4111, Australia
E-mail: moutoshi.chakraborty@griffithuni.edu.au

The ORCID identification number(s) for the author(s) of this article can be found under https://doi.org/10.1002/adsr.202400103

DOI: 10.1002/adsr.202400103

M. Chakraborty, S. Strachan, R. Ford
School of Environment and Science (ESC)
Griffith University
Nathan Campus, QLD 4111, Australia

S. A. Bhuiyan
Sugar Research Australia (SRA)
90 Old Cove Road, Woodford, QLD 4514, Australia

S. A. Bhuiyan, S. Strachan, N.-T. Nguyen, N. Soda
Queensland Micro- and Nanotechnology Centre (QMNC)
Griffith University
Nathan Campus, QLD 4111, Australia

M. J. Shiddiky
Rural Health Research Institute (RHRI)
Charles Sturt University
Orange, NSW 2800, Australia

sion of symptoms makes accurate and timely disease identification challenging. This has led to the global spread of LS through apparently "healthy" planting materials.[3] To address this, several LS diagnosis methods were developed, including isolation of the bacteria on selective media,[7] microscopy,[8] ELISA (Enzyme-Linked Immunosorbent Assay),[9] PCR (Polymerase Chain Reaction),[10] nested-PCR,[11] qPCR (Quantitative Polymerase Chain Reaction),[12] LAMP (Loop-mediated Isothermal Amplification),[13] and EC (Electrochemical) detection.[14] However, each of these methods has drawbacks. While isolation on selective media and microscopy can effectively detect *Xalb* in symptomless plants, they are labor-intensive and have low sensitivity.[8,9] Immunological, molecular, and electrochemical detection technologies provide varying levels of sensitivity. However, the requirement of sophisticated laboratory facilities and reliance on commercial kits or chemical-based multistep DNA extraction procedures limits their wide application. These challenges highlight the need for a simple, rapid, and cost-effective *Xalb* detection method requiring minimal or no chemical reagents for sample preparation.

To speed up the *Xalb* diagnostic process, a straightforward and rapid method involving heat-induced DNA isolation without the need for reagents can be evaluated. This approach would simplify the release of *Xalb* DNA by avoiding multiple processing steps and the need for commercial kits or chemicals.[15] High temperatures break down microorganism cell walls, releasing nuclear content.[14,16,17] Specifically, Jose and Brahmadathan[16] observed that heating to 94 °C for 2 min was adequate to denature bacterial cell walls. Previously, this method was used to extract bacterial nucleic acid from different biological materials.[18–20] When combined with electrochemical detection, this provides a straightforward approach for the identification and quantification of *Xalb*.

Electrochemical biosensors (EC) are rapid, cost-effective, PCR amplification-free platforms for plant pathogen detection.[21–25] Recently, Umer et al.[14] reported a reagent-free heat-induced DNA isolation method combined with a *Xalb* EC protocol. However, this process requires intricate sensor fabrication, presenting considerable challenges in developing a straightforward and user-friendly platform for pathogen testing. In this paper, a new approach has been introduced for the simple, sensitive, cost-effective, amplification-free, and sensor fabrication-free EC detection of *Xanthomonas albilineans* (*Xalb*) DNA from sugarcane samples. Our study aimed to develop an electrochemical LS diagnostic method that: i) is compatible with a straightforward one-step DNA isolation procedure; and ii) allows for amplification-free quantitative detection of *Xalb* DNA from sugarcane samples with sensitivity levels appropriate for routine diagnostics. We then aimed to iii) demonstrate the electrochemical quantification of *Xalb*-specific target DNA sequences in sugarcane leaf, meristematic tissue, and xylem sap samples.

2. Experimental Section

2.1. Source of Bacteria and Culture Conditions

The *Xalb* strain 3/14/9 was obtained from the Sugarcane Research Australia (SRA) Indooroopilly Research Station in Queensland, Australia (S 26.93 and E 152.78°). The bacterium was cultured in modified Wilbrink's broth media following Dawson's protocol.[26] To determine the specificity of the probe for the *Xalb* target sequence, the bacteria *Leifsonia xyli* subsp. *xyli* (*Lxx*), which causes ratoon stunting disease (RSD) of sugarcane,[27] and the fungus *Ceratocystis paradoxa* (*Cpar*), which causes sugarcane pineapple sett rot disease were used. *Lxx* was isolated from an infected sugarcane plant at the SRA Woodford Pathology Research Station in Queensland. It was cultured in a modified liquid broth S8 medium and incubated at 28 °C for 4 weeks, following the protocols outlined by Davis et al.[28] and Chakraborty et al.[15] *Cpar* was collected from the Woodford Pathology Research Station and cultured in potato dextrose agar media (PDA) at 28 °C for 5 days, following the method of Rahman et al.[29]

Table 1. List of sugarcane varieties and their leaf scald resistance ratings, categorized according to phenotypic symptoms.

Variety	LS rating	Rating category
Q68	1	Moderately resistant
Q208	1	Moderately resistant
Q124	2	Moderately resistant
Q133	4	Intermediate resistant
Q96	5	Intermediate resistant
Q63	6	Intermediate susceptible
Q87	7	Susceptible
Q44	9	Highly susceptible

2.2. Establishment of Field Trial, Inoculation, and Planting

The trial was carried out at the SRA Pathology Research Station in Woodford in September 2020. Eight sugarcane cultivars were obtained from a disease-free propagation block located at the same research station (**Table 1**). The one-budded set of each sugarcane cultivar was inoculated with *Xalb* on a cloudy day by a decapitation technique as described by Koike.[30] The study was conducted utilizing a randomized complete block (RCB) design, with three replications, and each replication contained six plants.

2.3. Sugarcane Field Samples

Sugarcane leaf, meristematic tissues, and xylem sap samples were collected from three stalks (one stalk per replication) at 53 weeks post-inoculation. Vascular extracts (2 mL per variety) were obtained using positive air pressure extraction, following the method described by Croft et al.[31], and stored at −20 °C until further processing. All the samples were collected from eight sugarcane varieties as described in Table 1. Each variety was previously assessed for LS disease resistance for multiple years by observing the visible symptoms (Table 1).

2.4. DNA Extraction

For electrochemical analysis, a rapid, reagent-free DNA isolation method was used, as described by Chakraborty et al.[15]. To create a titrated series (ranging from 10^6 to 10^0 cells μL^{-1}) for a standard curve of detection, cultured cells of *Xalb* were introduced

into disease-free xylem sap of sugarcane and subjected to boiling for 2 min at 95 °C in a heat block. Following the boiling step, 10 µL of supernatant was utilized directly as a template for EC analysis. In the case of infected field samples, leaf, and meristematic tissues were cut into tiny pieces and incubated in 100 µL of distilled water for 10 min. Subsequently, the sample solution was heat lysed, and 10 µL of the resulting supernatant was used for further analysis. For sap samples, 100 µL of sap underwent the same boiling process at 95 °C for 2 min on a heat block, and 10 µL of resulting supernatant was used for analysis. Each sample was replicated three times, and the entire experiment was carried out thrice to ensure accuracy and reliability.

Genomic DNA of *Xalb* from cultured cells and LS-infected sugarcane samples was extracted for qPCR analysis following the protocol outlined in The PureLink Microbiome DNA purification kit manual (Thermo Fisher Scientific, Australia). Each experiment was performed three times with three replications to maintain consistency.

2.5. Target Selection and Primer Design

A probe (*Xalb*CP1) was designed targeting a 34 bp region (Table S1, Supporting Information) within the gene cluster of *XALB1* albicidin pathotoxin biosynthesis. This region corresponded to positions 43171 to 43204 in the *X. albilineans* genome (GenBank accession no. AJ586576.1).[32] The selection of this target region was based on the significant role that albicidin plays in the pathogenesis of LS, as highlighted in previous studies.[33,34] Furthermore, it was noted that this region showed no significant similarity (E < 10) to other sequences available in the GenBank database.

For qPCR analysis, forward and reverse primers (*Lxx*FP and *Lxx*RP, see Table S1, Supporting Information) were designed using the NCBI primer blast web tool[35] to target a 196 bp segment within the same *XALB1* albicidin pathotoxin biosynthesis gene cluster of *Xalb*, corresponding to positions 43 128 to 43 323. The sequences of probes, primers, and the synthetic target sequence (STS_EC_ *Xalb*) are provided in Table S1 (Supporting Information). To confirm specificity, the probes, and each primer were screened against corresponding sequences using the BLASTn tool[36] against the NCBI nucleotide and genome databases, with all sequences exhibiting 100% homology to the respective *Xalb* sequences. The OligoAnalyzer Tool (Integrated DNA Technologies Inc., USA) was utilized to evaluate the potential formation of hairpins and dimers.

2.6. Probe Hybridization and Magnetic Isolation

To establish the concentrations of synthetic target sequences, the stock solution (100 µM) was diluted in nuclease-free water. Isolated DNA from serially diluted known numbers of *Xalb* cells and supernatants from heat-lysed sugarcane samples were used without further dilution. Each concentration underwent triplicate runs throughout the entire process, from capturing the target to detection. The target sequences were isolated and purified magnetically according to our previously established protocol.[37,38] The purified targets were then stored at −20 °C for subsequent EC quantification.

2.7. Sensor Fabrication and Assay Optimization

Electrodes were cleaned and allowed to air dry between each detection procedure. To enhance the assay sensitivity, the EC pretreatment method for screen-printed gold electrodes (SPGEs) was employed according to Zhang et al.[39] With cyclic voltammetry (CV) conditions, the peak current for the one-electron reduction of $[Fe(CN)_6]^{3-}$ was measured as a function of scan rate. The effective area of the working electrode was calculated by the Randles–Sevcik equation:[40]

$$i_p = 2.69 \times 10^5 n^{3/2} A D^{1/2} c v^{1/2} \quad (1)$$

where, i_p: the peak current (A); n: the number of electrons transferred ($Fe^{3+} \rightarrow Fe^{2+}$, $n = 1$); A: effective area of the working electrode (cm^2); D: diffusion coefficient of $[Fe(CN)_6]^{3-}$ (7.60×10^{-5} cm^2 s^{-1}); v: scan rate (V s^{-1}); and c: concentration (mol cm^{-3}).

Following the isolation of the target as previously described, 10 µL of the target-containing solution was directly deposited onto the gold nanoparticles (AuNPs) modified electrode surface. A constant potential of 0.6 V versus Ag/AgCl was applied, following published protocols.[41,42] To optimize the deposition of target DNA on the SPGE, experiments were conducted with various deposition potentials (−400 mV, +200 mV, +600 mV, and +800 mV) and deposition times (60, 120, 200, and 300 s). These experiments employed a synthetic target concentration for the DNA-gold adsorption process prior to the EC readout, as the charge conditions can significantly influence the deposition quantity. To optimize the EC performance of the AuNPs-SPGE, the optimal deposition potential and time for *Xalb* DNA adsorption were determined based on the maximum response obtained within the minimal duration. Unbound species were subsequently washed away three times with 10 mM PBS buffer solution.

2.8. Electrochemical Detection

For EC detection, a 2 mM ferricyanide solution was introduced to the SPGE-AuNP surface, and differential pulse voltammetry (DPV) measurements were taken with the following parameters: initial voltage −0.2 V, final voltage 0.45 V, and the amplitude 0.05 V. The quantity of *Xalb* DNA adsorbed onto the sensor surface was directly correlated with these measurements. The percent current response change was measured as follows:

$$\Delta i^* = \left[\left(i_{\text{Bare}} - i_{\text{Adsorbed}}\right) / i_{\text{Bare}}\right] \times 100 \quad (2)$$

where i_{Bare} and i_{Adsorbed} were the current densities for the bare electrode and the electrode after sample adsorption, respectively.

2.9. Validation with qPCR and Gel Electrophoresis

Electrochemical results were verified through a conventional qPCR approach using *Xalb* cell samples. To generate a standard plot for qPCR-based absolute quantification, cycle quantification (Cq) values were plotted against the log of the corresponding quantity of pure DNA extracted from a known number of *Xalb* cells (10^6–10° cells μL^{-1}) spiked into fresh sap samples. To validate the EC assay with field samples, qPCR experiments were

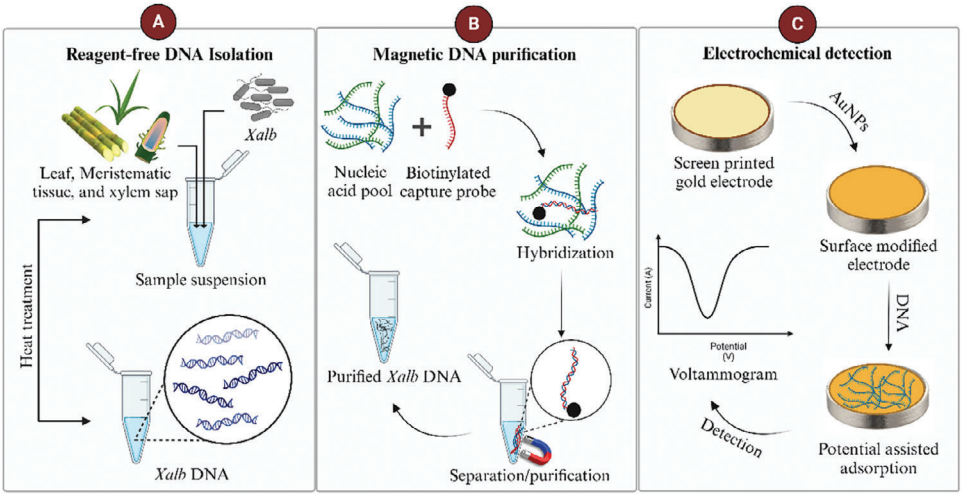

Figure 1. Schematic representation of the EC detection assay for *X. albilineans* DNA. The procedure involved: A) DNA isolation from samples utilizing a boiling lysis approach; B) specific capture of *Xalb* DNA using biotinylated DNA capture probes, followed by magnetic purification with streptavidin-coated magnetic beads, and subsequent release of *Xalb* DNA from magnetic beads, and C) potential-facilitated deposition onto gold nanoparticle-modified screen-printed gold electrodes for EC detection. The adsorption of *Xalb* DNA leads to increased coulombic repulsion of negatively charged ferricyanide ions thereby resulting in a reduction of the EC signal at the electrode surface.

performed using a conventional LS detection method that employs a commercial kit for the extraction and purification of *Xalb* DNA from LS-infected sugarcane samples. Infected leaf, meristematic tissues, and sap samples from eight sugarcane varieties collected from the SRA Woodford LS screening trial were analyzed. The qPCR reactions were set up following the manufacturer's instructions (New England Biolabs, USA) and carried out using a CFX96 Touch Real-Time PCR Detection System (Bio-Rad Laboratories Pty Ltd, Australia) with the following reaction conditions: the initial denaturation at 100 °C for 1 min; 40 cycles at 98 °C for 15 s, 52 °C for 30 s, and 72 °C for 30 s; followed by a final extension at 72 °C for 2 min and hold at 4 °C for 5 min. The cycle quantification (Cq) for each dilution was analyzed at the conclusion of the reaction, with the presence of *Xalb* confirmed if a positive result was observed within 40 cycles. Sterile distilled water was used as a no-target control, and each assay was conducted in triplicate for each repetition. PCR products were electrophoresed on a gel using a gel documentation system (Thermo Fisher Scientific, Australia) according to Chakraborty et al.[15] for further confirmation. Positive reactions were identified by the presence of a 196 bp product, as determined using the GeneRuler 100 bp ladder (Thermo Fisher Scientific, Australia).

2.10. Statistical Analysis

Data analysis for the EC was performed using OriginPro 2022 v.9.9.0.225 (OriginLab, Northampton, Massachusetts, USA), R programming language (version 4.2.1), and Microsoft Excel 365 (USA). A *Linear Mixed Model* was fitted to all data sets using *lmerTest::lmer* of R (version 4.3.1). In the model, replications and error terms (residuals) were considered as random effects, while the varieties were considered as fixed effects. Normality for log-transformed and untransformed data was tested using R's *qqnorm*, *qqline*, and *Shapiro-test* commands. Untransformed data showed reasonable normality, and no significant improvement in normality was observed in the log-transformed data; therefore, untransformed data were used for the analysis. For the appropriate significant factors, a protected mean comparison of all possible pairwise differences of the mean of Cq and EC values was tested at alpha = 0.05, using Fisher's protected LSD test. To calculate the Spearman correlations between EC value and qPCR value (Cq) or resistance ratings, *ggcorrmat* of R was used. Data visualizations were generated using BioRender, SnapGene software (www.snapgene.com), and Microsoft PowerPoint 365 (USA). The figures depict mean values with standard error bars, derived from three independent replications.

3. Results and Discussion

3.1. Assay Design

The process of the newly developed *Xalb* detection assay is depicted in **Figure 1**. Initially, bacterial DNA was released from sugarcane samples utilizing a simple lysis boiling-based technique (Figure 1A). Subsequently, the *Xalb*-targeted complementary biotinylated capture was performed using the *Xalb*CP1 probe attached to the surface of magnetic beads coated with streptavidin. The captured *Xalb* targets were then purified through magnetic separation and washing steps to remove non-targets while retaining the nanoparticle/capture probe/target complexes. The *Xalb* targets were subsequently released from the capture probe/nanoparticle complexes by heat, allowing the probe-bound target sequences to be extracted from the solution (Figure 1B). The released *Xalb* targets were then adsorbed onto the modified metal surface via the gold-DNA affinity interaction. Finally, EC detection was conducted by voltametric interrogation with $[Fe(CN)_6]^{3-}$ to acquire differential pulse voltammetry (DPV) readout for quantifying the captured target (Figure 1C). The adsorbed *Xalb* DNA reduced the EC signal due to increased

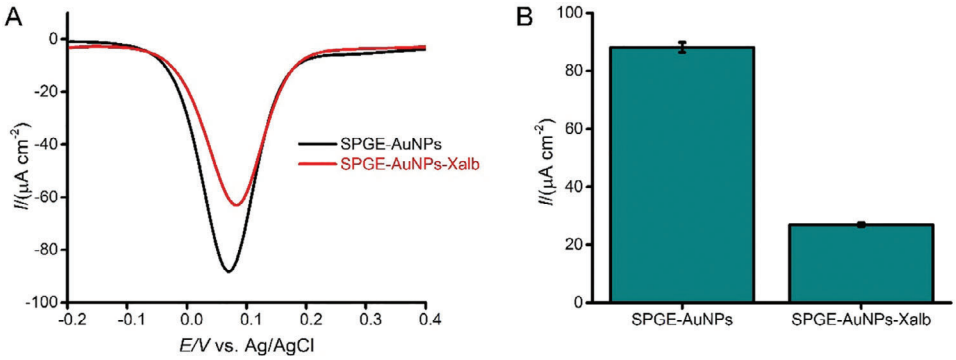

Figure 2. The current densities were obtained during the assessment of assay functionality using a synthetic target (1 pM). A) Displays the differential pulse voltammograms, while B) presents the mean percentage change in current response corresponding to the presence and absence of the target on the AuNPs modified electrode. Each error bar is the mean of three replications and depicts the standard deviation (SD) of each independent experiment (SD <5%; $n = 3$).

coulombic repulsion of negatively charged ferricyanide ions away from the surface of the electrode.[40]

3.2. Assay Optimization

To enhance assay sensitivity, the SPGE surface was modified with gold nanoparticles (AuNPs), resulting in a nearly doubled current density response (average current density 8.80 vs 3.91 mA cm^{-2}; $n = 3$) (Figure S1, Supporting Information). AuNPs are known for their high conductivity, aiding swift electron transfer between the electrolytic solution and the transducer, a technique employed in prior studies.[43–49] This modification aimed to reduce the surface impedance of the working electrode, enabling the detection of minute changes in electron transfer at the interface.[50] AuNPs are preferred due to their high biocompatibility and ability to maintain the activity of biological molecules over time.[51–53]

For precise target binding and quantification, the optimal potential and deposition times for *Xalb* DNA adsorption were determined as +600 mV and 60 s, respectively (Figures S2, S3, Supporting Information). The performance of the assay was assessed with and without synthetic *Xalb* targets to determine its functionality (**Figure 2**). The adsorption of negatively charged entities onto the gold sensor surface via DNA-gold affinity interactions led to coulombic repulsion with ferricyanide ions. In contrast to the no-target control, this repulsive force caused the one-electron transfer reaction's faradaic current signal to decrease.[54]

3.3. Assay Sensitivity and Specificity

Increasing *Xalb* concentrations led to a reduced current signal during DPV, attributed to more target molecules blocking the sensor surface.[55] This increased *Xalb* adsorption caused greater coulombic repulsion of $[Fe(CN)_6]^{3-}$ ions, hindering their diffusion to the surface of the electrode and reducing the Faradaic current. Sensitivity was evaluated from 1 nM to 1 fM, showing a linear calibration plot with a regression equation of $y = 5.72$ logC + 1.64 (where y is the change in current and C is the *Xalb* concentration), and a correlation coefficient (r) of 0.99 (**Figure 3** inset). Compared to the no-template control (NTC), which had an unblocked sensor surface and high current reading, our assay detected *Xalb* targets down to 1 fM with reproducibility of SD ≤ 5% for $n = 3$.

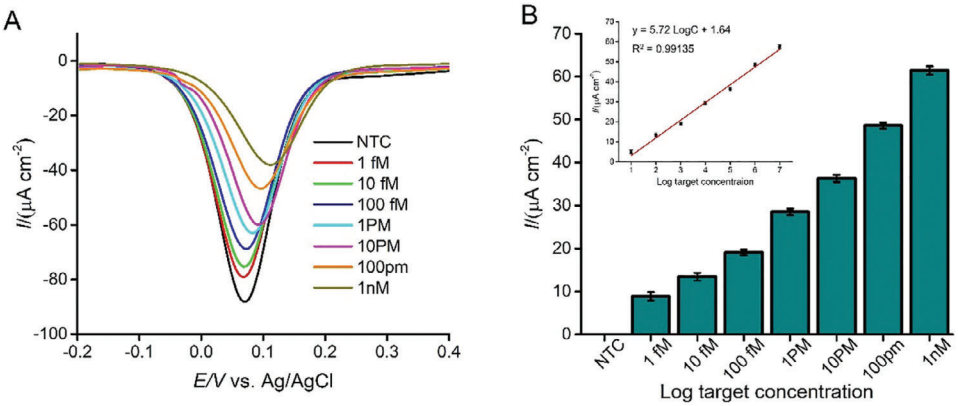

Figure 3. Sensitivity analysis. A) Current densities were measured for known synthetic target concentrations (1nM–1fM) compared to the NTC. Each error bar is the mean of three replications and depicts the standard deviation (SD) of each independent experiment (SD <5%; $n = 3$). B) A corresponding bar graph illustrates synthetic target detection. An inset shows a calibration plot demonstrating the concentration-current density relationship.

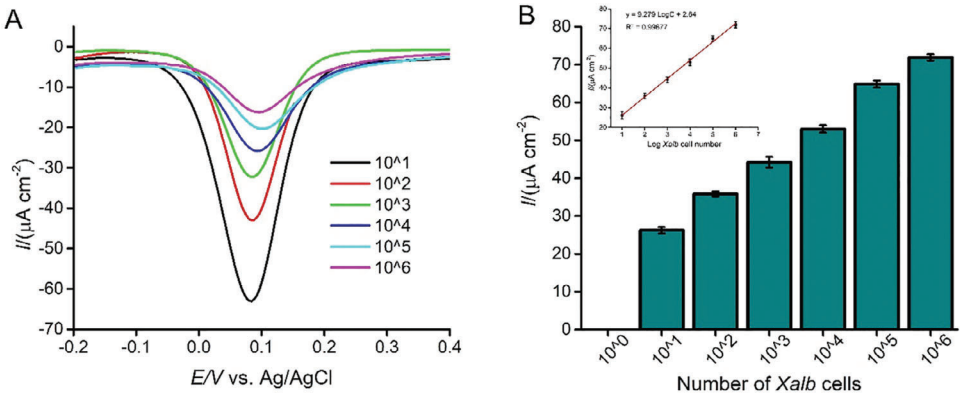

Figure 4. Sensitivity of assay with *Xalb* cells. A) Differential pulse voltammograms correspond to input total DNA from known numbers of *Xalb* cells. B) Mean % current response change using input total DNA from different numbers of *Xalb* cells. An inset displays the corresponding linear calibration plot. Each error bar is the mean of three replications and depicts the standard deviation (SD) of each independent experiment (SD <5%; $n = 3$).

This newly developed EC assay demonstrated sensitivity exceeding that of a recently developed *Xalb* diagnosis platform by 100 times, surpassing reported detection limits in the range of 100 fM[14], all without the need for complex sensor fabrication processes. Although Siddiquee et al.[56] presented a platform demonstrating attomolar-level sensitivity with detection across an extensive dynamic range (1.0×10^{-18} to 1.82×10^{-4} mol L^{-1}), surpassing our assay in sensitivity, this involved intricate sensor fabrication and relied on a labor-intensive phenol-chloroform-based DNA extraction process. In contrast, our assay provides a straightforward, cost-effective, and quantitative result, facilitated by a user-friendly DNA isolation method suitable for field application, while eliminating the need for complex sensor fabrication steps. Importantly, our assay does not require target amplification/extension, labeling, or the use of antibodies. To ensure reliable quantification of *Xalb*, it is essential to establish a quantitative relationship between the EC signal and *Xalb* concentration, as well as to achieve a comprehensive detection range.

Therefore, to evaluate the assay's performance, EC detection was carried out using bacterial samples by introducing known concentrations of *Xalb* cells (ranging from 10^6 to 10^0 cells μL^{-1}) into fresh and uncontaminated sugarcane sap. The DPV responses showed a robust linear relationship across the titrated target concentrations (**Figure 4**). In comparison to the NTC, a significant change in the current response was observed with increasing target concentrations, demonstrating the assay's ability to detect *Xalb* sequences. Moreover, the assay demonstrated a dynamic range spanning five orders of magnitude, enabling the quantification of *Xalb* in sap samples with extremely diverse pathogenic loads. Accordingly, *Xalb* was detected at concentrations as low as 10 cells (Figure 4), presenting a simple and robust diagnostic method compared to several other reported EC methods.[21,25]

During specificity testing against other sugarcane pathogen contaminants, *Lxx* and *Cpar*, a marginal decrease in current response was observed (2.17 and 1.19 µA, respectively) compared to the NTC (**Figure 5**). This result indicates robust specificity for *Xalb*. In contrast, the presence of *Xalb* resulted in a two-fold lower current response compared to the no-target control (5.82 µA) (Figure 5). These findings suggest that the proposed biosensor demonstrates promising specificity for *Xalb* detection and holds considerable potential for biological applications.

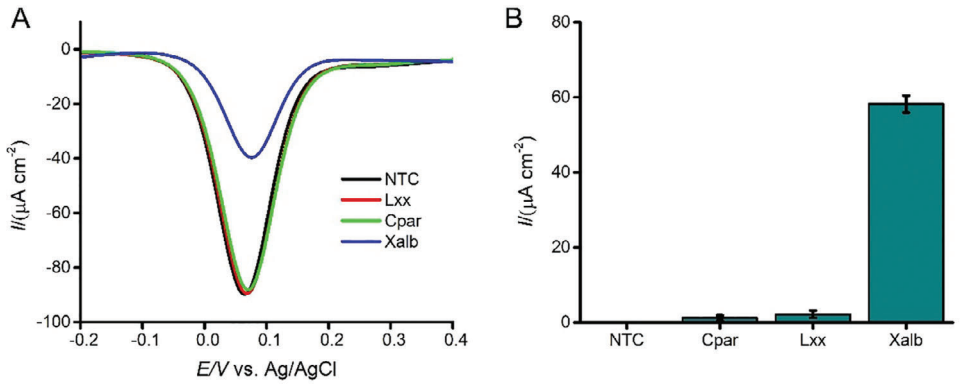

Figure 5. Specificity of assay. A) Differential pulse voltammograms for input DNA from *Xalb* cells, *Lxx* cells, and *Cpar* cells. B) Mean % current response change using input DNA from *Xalb* cells, *Lxx* cells, and *Cpar* cells. Each error bar is the mean of three replications and depicts the standard deviation (SD) of each independent experiment (SD <5%; $n = 3$). NTC stands for no target control; NG1 is the negative control with *Lxx* cells; NG2 is the negative control with *Cpar* cells.

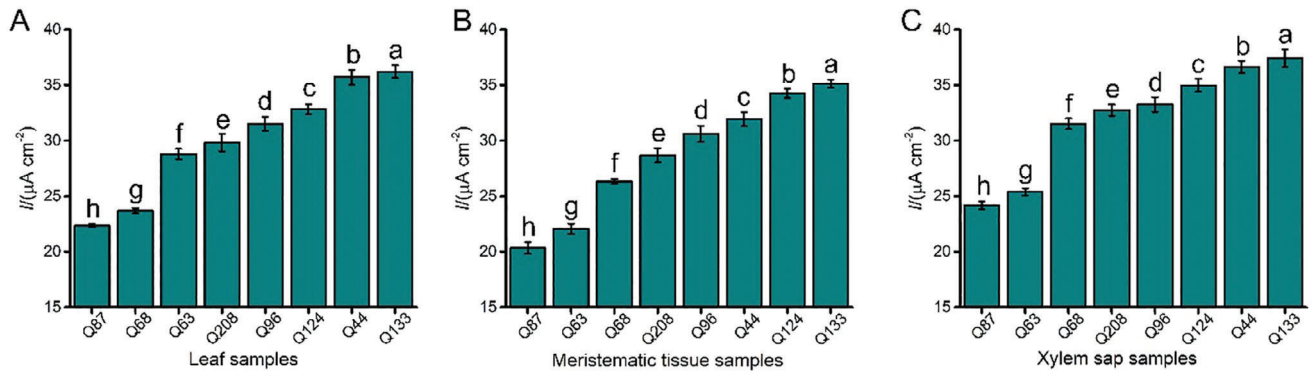

Figure 6. The bar graphs display current density measurements for all analyzed samples collected from SRA Woodford LS screening trials. Each bar is the mean of two replications, and bars with the same letter(s) are not significantly different using Fisher's protected LSD test ($p = 0.05$). Error bars depict the standard deviation (SD) of each mean.

To assess reproducibility, the assay's standard deviation of electrode measurements was found to be less than 5% ($n = 3$), indicating a high level of reliability. Traditional nucleic acid biosensors often rely on the specific binding of targets to complementary probes attached to a transducer or electrode surface. However, this 2D capture method can be susceptible to interference from non-specific molecules. In contrast, our method involves the selective capture of target *Xalb* DNA using complementary probes, followed by DNA isolation through magnetic bead separation. The subsequent magnetic washing and purification steps effectively remove matrix effects and significantly diminish non-specific interference.

3.4. Detection of *Xalb* in Different Sugarcane Samples

The newly developed *Xalb* EC biosensor was utilized to detect varying amounts of *Xalb* in leaf, meristematic tissue, and xylem sap samples from eight sugarcane cultivars derived from the LS field trial. Most samples exhibited *Xalb* DNA levels within the assay's detection threshold (1 fM), underscoring its practicality for real-world applications. The detected *Xalb* DNA levels in the various sugarcane samples were found to correlate with the bacterial loads. For instance, samples from Q87 and Q63 varieties showed relatively low current responses, indicating a lower bacterial presence in the leaf, meristematic tissue, and xylem (**Figure 6**). Similarly, cultivars Q68, Q208, Q44, Q96, Q124, and Q133 exhibited a gradual increase in the current responses, indicating a higher bacterial load in the sugarcane samples (Figure 6). This data demonstrates that the new electrochemical (EC) method is effective in detecting and quantifying *Xalb* titers in the infected sugarcane samples across various cultivars, regardless of their resistance status.

3.5. Validation with qPCR

A strong correlation was found between the EC and qPCR quantifications, confirming the new biosensor's effectiveness in detecting *Xalb* (**Figure 7**). qPCR successfully amplified the target *XALB1* albicidin pathotoxin biosynthesis gene cluster region from DNA extracted from as low as 100 cells. The gel exhibited clear and distinct bands of qPCR amplicons at the expected size for each corresponding sample (Figure S4, Supporting Information). No amplification or bands were seen in the NTC reaction during the analysis. The high correlation ($r = -0.95$–0.97, $p < 0.001$; **Tables 2**, **3**, and **4**) between the Cq values of EC and qPCR reactions confirmed the test's reliability. These outcomes demonstrate that the proposed EC assay has ten times more sensitivity than qPCR (Figure 4 vs Figure 7A). In further validation with field samples, qPCR successfully amplified the target region in all analyzed samples, demonstrating variations in pathogen loads, and detection sensitivity (Figure 7B–D). It showed a similar detection trend to our EC assay (Figure 6). In the gel, all analyzed samples showed clear bands as a positive response (Figure S5, Supporting Information). NTC showed no amplification or bands in any of the analyses. There was a significant correlation

Table 2. Spearman correlation coefficients using derived EC and qPCR data for comparing LS resistance ratings in leaf samples of eight sugarcane cultivars.

Factors[a)]	qPCR	Resistance rating
EC [b)]	0.95***	−0.12
qPCR[c)]		−0.05

[a)] Correlations were based on 24 observations, *** = significant at or <0.001 levels; [b)] EC = EC data from isolated DNA of leaf samples by heat-induced cell lysis; [c)] qPCR = qPCR data from commercial kit-based DNA extraction of leaf samples.

Table 3. Spearman correlation coefficients using derived EC and qPCR data for comparing LS resistance ratings in meristematic tissue samples of eight sugarcane cultivars.

Factors[a)]	qPCR	Resistance rating
EC [b)]	0.97***	0.13
qPCR[c)]		−0.01

[a)] Correlations were based on 24 observations, *** = significant at or <0.001 levels; [b)] EC = EC data from isolated DNA of meristematic tissue samples by heat-induced cell lysis; [c)] qPCR = qPCR data from commercial kit-based DNA extraction of meristematic tissue samples.

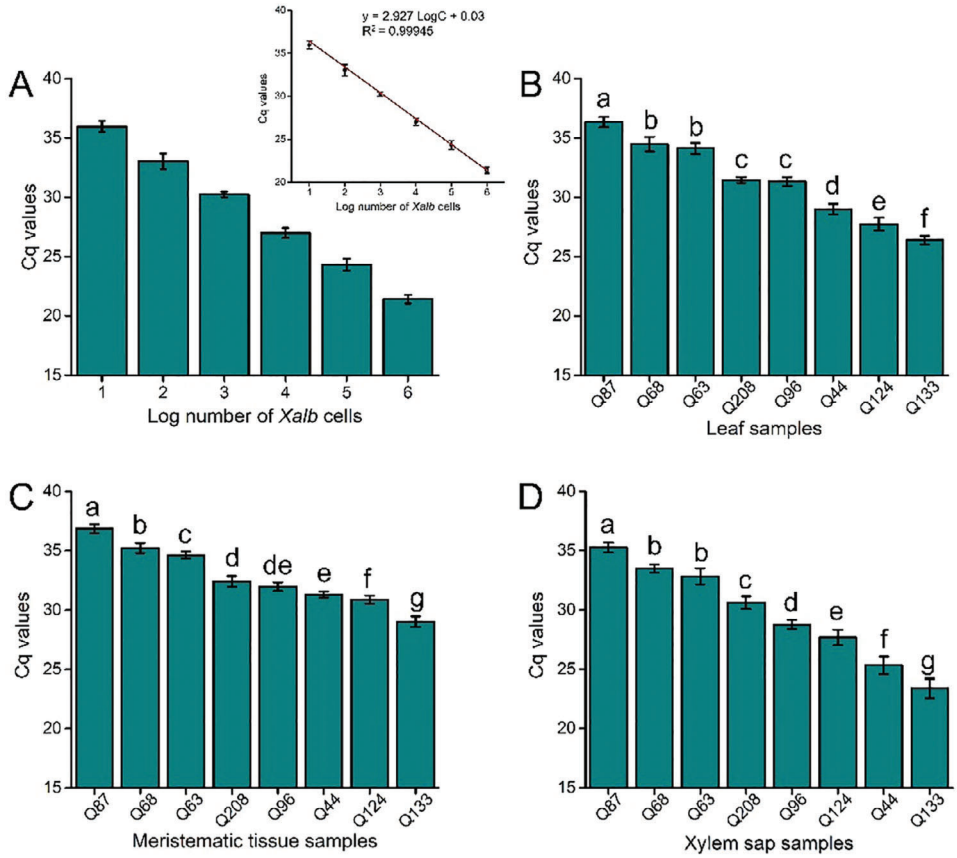

Figure 7. Validation of the assay using qPCR. Initial quantity for A) a known number of *Xalb* cells (10^6–10° cells μL^{-1}), and a set of LS infected B) leaf, B) meristematic tissues, and B) xylem sap samples as assessed by qPCR-based absolute target quantification. Each bar is the mean of two replications, and bars with the same letter(s) are not significantly different using Fisher's protected LSD test ($p = 0.05$). Error bars depict the standard deviation (SD) of each mean.

($r = -0.95$–0.97, $p < 0.001$) between the qPCR values of all samples and the results of the biosensor assay according to Tables 2, 3, and 4. The strong correlation ($r = -0.95$-0.97, $p < 0.001$) between the EC current response and Cq values of both biosensor and qPCR samples confirmed the reliability of the EC test. However, there was no correlation between the qPCR and EC values for leaf ($r = -0.12$ and -0.05), meristematic tissue ($r = 0.13$ and -0.01), and xylem sap samples ($r = 0.03$ and -0.12) with the LS resistance rating (Tables 2,3, and 4).

This suggests that *Xalb* may be effectively detected and quantified in leaf, meristematic, and xylem sap samples using our assay's EC signals. In negative controls, EC signals were comparable to background signals, with a <10% change in the current response, confirming assay specificity. The successful application of our assay to real biological samples (Figure 6) and subsequent validation through qPCR (Figure 7), alongside gel analysis of qPCR products, highlights the technique's suitability for biological use. Our study revealed that there is little correlation between qPCR or EC values and the resistance ratings of different sugarcane cultivars. This differs from previous findings in the USA, where the qPCR values demonstrated a moderate correlation with the resistance categories of the sugarcane cultivars.[12,57] A key difference between these two studies is that the correlations in the USA study were based on visual symptom ratings and qPCR values, while in our study, the correlations were established using qPCR or EC values along with historical disease ratings for the cultivars.

Meanwhile, the bacterial load in sugarcane cultivars may vary depending on the number of bacteria used for inoculation. Gutierrez et al.[57] demonstrated that severe inoculation resulted in moderate to high bacterial populations in resistant cultivars. Our earlier research indicated that bacterial populations in sap samples are not a reliable indicator of resistance to LS disease (Chakraborty et al., unpublished data). Furthermore, it was observed that the bacterial populations in younger leaves exhibited

Table 4. Spearman correlation coefficients using derived EC and qPCR data for comparing LS resistance ratings in sap samples of eight sugarcane cultivars.

Factors[a]	qPCR	Resistance rating
EC[b]	0.95***	0.03
qPCR[c]		−0.12

[a] Correlations were based on 24 observations, *** = significant at or <0.001 levels; [b] EC = EC data from isolated DNA of xylem sap samples by heat-induced cell lysis; [c] qPCR = qPCR data from commercial kit-based DNA extraction of xylem sap samples.

the most significant differences between resistant and susceptible cultivars.[12] However, further investigations are needed to understand the relationships between cultivar resistance and bacterial population in sugarcane plants, especially in relation to the age and location of plant parts.

4. Conclusion

This proof-of-concept study reports a highly sensitive approach to identifying *X. albilineans*, the causal agent of sugarcane leaf scald disease. The method enables the use of electrochemical methods to quantify *Xalb* at femtomolar DNA levels. The test exhibits remarkable specificity, with a strong linear response ($r = 0.99$) in the 1fM–1 nM target concentration range. It also shows outstanding reproducibility, with a sample size of three ($n = 3$) and a standard deviation (SD) of <5%. This assay offers several significant advantages. First, it is compatible with a low-cost boiling lysis-based DNA isolation technique that requires only basic tools, such as a heat block. The extracted DNA can then be sent to remote laboratories for testing. Additionally, the EC assay utilizes disposable electrodes, which cost as little as US$5 each, resulting in a per-sample cost of less than $10. Importantly, this method achieves high sensitivity in target detection without the need for complex sensor fabrication steps, distinguishing it from many previous EC assays.

This versatile technology holds the potential for broader application across various pathogens by employing specific probes. Beyond sugarcane, the assay could be beneficial for managing and identifying diseases in horticulture and other agricultural crops, as well as in diverse environments, including soil. Furthermore, multiplexing or high-throughput detection of multiple pathogens simultaneously is achievable by utilizing multiwell screen-printed electrodes. The assay's adaptability makes it a strong candidate for developing a fully integrated, next-generation handheld device for on-farm use, supported by a dedicated smartphone application. This device might be useful in establishing geographic information systems (GIS) for disease surveillance, prevalence assessment, and risk mapping. Furthermore, this integrated device may be essential to the implementation of rapid exotic disease detection and warning systems, especially at high-risk entry sites like seaports and airports.

Supporting Information

Supporting Information is available from the Wiley Online Library or from the author.

Acknowledgements

The supply of infected and clean plant materials from Sugar Research Australia is gratefully acknowledged. The Australian Research Council Linkage Project (LP200100016) supplied the operating funds for this work, with further resources from Sugar Research Australia (SRA). The lead author received a Griffith University International Postgraduate Research Scholarship and a PhD Competitive Research Grant from the Centre for Planetary Health and Food Security (CPHFS) of Griffith University.

Conflict of Interest

The authors declare no conflict of interest.

Data Availability Statement

The data that support the findings of this study are available from the corresponding author upon reasonable request.

Keywords

affinity interaction, biosensing, biosensor, electrochemical detection, nucleic acid isolation, sugarcane leaf scald disease

Received: July 5, 2024
Revised: October 18, 2024
Published online:

[1] L. H. Lin, M. S. Ntambo, P. C. Rott, Q. N. Wang, Y. H. Lin, H. Y. Fu, S. J. Gao, *Crop Prot.* **2018**, *109*, 17.
[2] P. Rott, M. Davis, *A Guide to Sugarcane Diseases*, (Eds.: P. Rott, R. A. Bailey, J. C. Comstock, B. J. Croft, A.S. Saumtally), CIRAD/ISSCT, Montpellier, France **2000**.
[3] P. Rott, I. S. Mohamed, P. Klett, D. Soupa, A. de Saint-Albin, P. Feldmann, P. Letourmy, *Phytopathology* **1997**, *87*, 1202.
[4] P. Rott, M. Marguerettaz, L. Fleites, S. Cociancich, J. C. Girard, I. Pieretti, D. W. Gabriel, M. Royer, *Proc. Int. Soc. Sugar Cane Technol.* **2010**, *27*, 490.
[5] P. Champoiseau, P. Rott, J. H. Daugrois, *Plant Dis.* **2009**, *93*, 339.
[6] J. H. Daugrois, R. Boisne-Noc, P. Champoiseau, P. Rott, *Funct. Plant Sci. Biotechnol.* **2012**, *6*, 91.
[7] M. J. Davis, P. Rott, P. Baudin, J. L. Dean, *Plant Dis.* **1994**, *78*, 78.
[8] I. Mensi, M. S. Vernerey, D. Gargani, M. Nicole, P. Rott, *Open Biol.* **2014**, *4*, 130116.
[9] Z. K. Wang, J. C. Comstock, E. Hatziloukas, N. W. Schaad, *Plant Pathol.* **1999**, *48*, 245.
[10] Y. B. Pan, M. P. Grisham, D. M. Burner, *Plant Dis.* **1997**, *81*, 189.
[11] M. J. Davis, P. Rott, G. Astua-Monge, *Phytopathology* **1998**, *88*, 1372.
[12] F. F. Garces, A. Gutierrez, J. W. Hoy, *Plant Dis.* **2014**, *98*, 121.
[13] D. V. Dias, E. Fernandez, M. G. Cunha, I. Pieretti, M. Hincapie, P. Roumagnac, J. C. Comstock, P. Rott, *Trop. Plant Pathol.* **2018**, *43*, 351.
[14] M. Umer, N. B. Aziz, S. Al Jabri, S. A. Bhuiyan, M. J. Shiddiky, *Crop Pasture Sci.* **2021**, *72*, 361.
[15] M. Chakraborty, S. Bhuiyan, S. Strachan, S. Saha, R. Mahmudunnabi, N. T. Nguyen, M. Shiddiky, R. Ford, *Crop Pasture Sci.* **2024**, *75*, CP24053.
[16] J. J. M. Jose, K. N. Brahmadathan, *Indian J. Med. Microbiol.* **2006**, *24*, 127.
[17] S. Merk, H. Meyer, I. Greiser-Wilke, L. Sprague, H. Neubauer, *J. Vet. Med., Ser. B* **2006**, *53*, 281.
[18] A. A. Dashti, M. M. Jadaon, A. M. Abdulsamad, H. M. Dashti, *Kuwait Med. J.* **2009**, *41*, 117.
[19] M. Ghai, V. Singh, L. A. Martin, S. A. McFarlane, T. van Antwerpen, R. S. Rutherford, *Lett. Appl. Microbiol.* **2014**, *59*, 648.
[20] I. Smyrlaki, M. Ekman, A. Lentini, N. Rufino de Sousa, N. Papanicolaou, M. Vondracek, J. Aarum, H. Safari, S. Muradrasoli, A. G. Rothfuchs, J. Albert, B. Högberg, B. Reinius, *Nat. Commun.* **2020**, *11*, 4812.
[21] P. Wongkaew, S. Poosittisak, *Am. J. Plant Sci.* **2014**, *5*, 2256.
[22] Y. Fang, R. P. Ramasamy, *Biosensors* **2015**, *5*, 537.
[23] M. Khater, A. de la Escosura-Muñiz, A. Merkoci, *Biosens. Bioelectron.* **2017**, *93*, 72.
[24] E. E. Ferapontova, *Annu. Rev. Anal. Chem.* **2018**, *11*, 197.
[25] L. Jiang, L. Luo, Z. Zhang, C. Kang, Z. Zhao, D. Chen, Y. Long, *Talanta* **2024**, *268*, 125336.

[26] W. J. Dawson, *Plant Diseases Due to Bacteria*, 2nd ed., Vol. *1*, Cambridge University Press, Cambridge, **1957**, p. 48.
[27] M. Chakraborty, N. Soda, S. Strachan, C. N. Ngo, S. A. Bhuiyan, M. J. Shiddiky, R. Ford, *Phytopathology* **2024**, *114*, 7.
[28] M. J. Davis, A. G. Gillaspie Jr, R. W. Harris, R. H. Lawson, *Science* **1980**, *210*, 1365.
[29] M. A. Rahman, M. F. Begum, M. F. Alam, *Mycobiology* **2009**, *37*, 277.
[30] H. Koike, *Phytopathology* **1965**, *55*, 317.
[31] B. J. Croft, A. D. Greet, T. M. Lehmann, D. S. Teakle, *Proc. Aust. Soc. Sugar Cane Technol.* **1994**, *16*, 143.
[32] N. C. B. Information, (NCBI), Leifsonia xyli subsp. xyli str. CTCB07, complete genome, Accession No. AE016822, National Library of Medicine (US), Bethesda (MD) **1988**.
[33] M. Royer, L. Costet, E. Vivien, M. Bes, A. Cousin, A. Damais, I. Pieretti, A. Savin, S. Megessier, M. Viard, R. Frutos, *Mol. Plant Microbe Interact.* **2004**, *17*, 414.
[34] I. Pieretti, M. Royer, V. Barbe, S. Carrere, R. Koebnik, S. Cociancich, A. Couloux, A. Darrasse, J. Gouzy, M.-A. Jacques, E. Lauber, C. Manceau, S. Mangenot, S. Poussier, B. Segurens, B. Szurek, V. Verdier, M. Arlat, P. Rott, *BMC Genomics* **2009**, *10*, 616.
[35] J. Ye, G. Coulouris, I. Zaretskaya, I. Cutcutache, S. Rozen, T. L. Madden, *BMC Bioinf.* **2012**, *13*, S1.
[36] Y. Chen, W. Ye, Y. Zhang, Y. Xu, *Nucleic Acids Res.* **2015**, *43*, 7762.
[37] K. M. Koo, N. Soda, M. J. Shiddiky, *Curr. Opin. Electrochem.* **2021**, *25*, 100645.
[38] K. Clack, N. Soda, S. Kasetsirikul, R. Kline, C. Salomon, M. J. Shiddiky, *Biosensors* **2022**, *12*, 287.
[39] J. Zhang, S. Song, L. Wang, D. Pan, C. Fan, *Nat. Protoc.* **2007**, *2*, 2888.
[40] M. J. A. Shiddiky, A. A. J. Torriero, C. Zhao, I. Burgar, G. Kennedy, A. M. Bond, *J. Am. Chem. Soc.* **2009**, *131*, 7976.
[41] K. K. Leung, H. Z. Yu, D. Bizzotto, *ACS Sens.* **2019**, *4*, 513.
[42] K. K. Leung, I. Martens, H. Z. Yu, D. Bizzotto, *Langmuir* **2020**, *36*, 6837.
[43] O. D. Renedo, M. J. A. Martínez, *Anal. Chim. Acta* **2007**, *589*, 255.
[44] S. Guo, E. Wang, *Anal. Chim. Acta* **2007**, *598*, 181.
[45] X. Cao, Y. Ye, S. Liu, *Anal. Biochem.* **2011**, *417*, 1.
[46] D. Davis, X. Guo, L. Musavi, C.-S. Lin, S.-H. Chen, V. C. H. Wu, *Ind. Biotechnol.* **2013**, *9*, 31.
[47] Y. Wang, E. C. Alocilja, *J. Biol. Eng.* **2015**, *9*, 16.
[48] L. Tian, L. Liu, Y. Li, Q. Wei, W. Cao, *Sci. Rep.* **2016**, *6*, 30849.
[49] M. Khater, A. de la Escosura-Muñiz, D. Quesada-González, A. Merkoçi, *Anal. Chim. Acta* **2019**, *1046*, 123.
[50] E. P. Randviir, *Electrochim. Acta* **2018**, *286*, 179.
[51] R. Shukla, V. Bansal, M. Chaudhary, A. Basu, R. R. Bhonde, M. Sastry, *Langmuir* **2005**, *21*, 10644.
[52] Y. Li, S. Xu, H. J. Schluesener, *Gold Bull.* **2010**, *43*, 29.
[53] J. Pengfei, Y. Wang, L. Zhao, C. Ji, D. Chen, L. Nie, *Nanomaterials* **2018**, *8*, 977.
[54] M. N. Islam, M. K. Masud, M. H. Haque, M. S. Al Hossain, Y. Yamauchi, N. T. Nguyen, M. J. A. Shiddiky, *Biosens. Bioelectron.* **2017**, *1*, 15.
[55] K. Murugappan, U. Sundaramoorthy, A. M. Damry, D. R. Nisbet, C. J. Jackson, A. Tricoli, *JACS Au* **2022**, *2*, 2481.
[56] S. Siddiquee, K. Rovina, N. A. Yusof, K. F. Rodrigues, S. Suryani, *Sens. Bio-Sens. Res.* **2014**, *2*, 16.
[57] A. Gutierrez, F. F. Garces, J. W. Hoy, *Plant Dis.* **2016**, *100*, 1331.